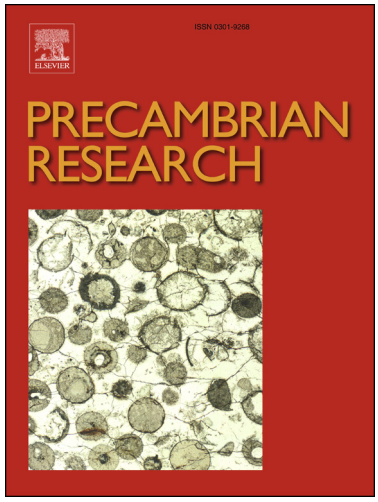

Stable isotopes of oxygen and hydrogen in meteoric water during the Cryogenian Period

Alasdair Skelton, Linda Löwhagen, Ian J. Fairchild, Adrian Boyce, Carl-Magnus Mörth, Heike Siegmund, David Webster, Anthony M. Spencer

PII: S0301-9268(18)30370-X
DOI: https://doi.org/10.1016/j.precamres.2018.11.006
Reference: PRECAM 5205

To appear in: *Precambrian Research*

Received Date: 11 July 2018
Revised Date: 25 September 2018
Accepted Date: 11 November 2018

Please cite this article as: A. Skelton, L. Löwhagen, I.J. Fairchild, A. Boyce, C-M. Mörth, H. Siegmund, D. Webster, A.M. Spencer, Stable isotopes of oxygen and hydrogen in meteoric water during the Cryogenian Period, *Precambrian Research* (2018), doi: https://doi.org/10.1016/j.precamres.2018.11.006

Stable isotopes of oxygen and hydrogen in meteoric water during the Cryogenian Period

Alasdair Skelton[a], Linda Löwhagen[a], Ian J. Fairchild[b], Adrian Boyce[c], Carl-Magnus Mörth[a], Heike Siegmund[a], David Webster[a] and Anthony M. Spencer[d]

[a] Department of Geological Sciences, Stockholm University, 106 91 Stockholm, Sweden

[b] School of Geography, Earth and Environmental Sciences, Birmingham University, Birmingham B15 2TT, UK

[c] Scottish Universities Environmental Research Centre, East Kilbride G75 0QF, UK

[d] Madlavollveien 14, 4041 Hafrsfjord, Norway

ABSTRACT

We measured $\delta^{18}O$ and $\delta^{2}H$ values of muscovite and carbonate mineral separates from metamorphosed carbonate-bearing mudstone layers in late Tonian to early Cryogenian strata, including Sturtian glacial deposits, which were deposited in a coastal setting at an approximate paleolatitude of 30-35°S and now crop out on Islay and the Garvellach Islands, Scotland. From these values, we calculated $\delta^{18}O$ and $\delta^{2}H$ values of meteoric water that equilibrated with clay at diagenetic conditions which we infer were reached shortly after deposition (i.e. before the end of the Cryogenian Period) because sediment accumulation was rapid due to fast subsidence at that time. This calculation required removal of the effects of exchange with reservoir rocks, metamorphic volatilization and mixing with metamorphic fluids on $\delta^{18}O$ and $\delta^{2}H$ values. The values we calculated for meteoric water fall within the 2σ ranges $\delta^{18}O$ = -1 to -4 ‰ and $\delta^{2}H$ = 0 to -23 ‰, respectively. These ranges are similar to present day values at equivalent latitudes. This finding is consistent with sediment accumulation in the Cryogenian Period having occurred in a climate similar to present day (Ice Age) conditions. This conclusion is not at odds with the Snowball Earth hypothesis because one of its predictions is that sediment accumulation occurred as the climate warmed at the end of panglaciation, a prediction supported by sedimentological evidence of multiple glacial advances and retreats in our study area and elsewhere.

1. Introduction

The $\delta^{18}O$ and $\delta^{2}H$ values of meteoric water can be used as a proxy for latitude, altitude and temperature (Craig, 1961; Dansgaard, 1964). This is because $\delta^{18}O$ and $\delta^{2}H$ values of meteoric water reflect condensation temperature and rainout of the airmass (Dansgaard, 1964). The $\delta^{18}O$ and $\delta^{2}H$ values of meteoric water in the past can be calculated from $\delta^{18}O$ and $\delta^{2}H$ values of minerals in rocks using mineral-water isotope fractionation factors (Bindeman and Serevyakov, 2011). However, unravelling original $\delta^{18}O$ and $\delta^{2}H$ values of meteoric water can be hampered by post-depositional exchange with reservoir rocks (Sheppard, 1986), metamorphic volatilization (Valley, 1986) and exchange with metamorphic fluids (Bickle and McKenzie, 1987). In this study, we sequentially remove the effect of each of these processes on $\delta^{18}O$ and $\delta^{2}H$ values measured on muscovite and carbonate separates from rocks exposed on Islay and the Garvellach Islands, western Scotland (Thomson, 1871; Spencer, 1971; Fairchild et al., 2018). These were deposited at an approximate paleolatitude of 30-35°S (Li et al., 2013) before, during and after early Cryogenian (Sturtian) glaciation and were subsequently metamorphosed at greenschist-facies conditions. In our study area, metamorphic fluid flow has been shown to have been spatially restricted due to structural channelization of the metamorphic fluids (Skelton et al., 2015). Those $\delta^{18}O$ and $\delta^{2}H$ values which have been affected by metamorphic fluid flow can thus be identified and removed. The effect of metamorphic volatilization can be calculated and removed by assuming that modification occurred by Rayleigh isotope fractionation (Valley, 1986). The $\delta^{18}O$ and $\delta^{2}H$ values of pore water in equilibrium with clay minerals can then be calculated using experimentally determined isotope fractionation factors and following the approach outlined by Fallick et al. (1993). By applying this approach, we revealed an array of $\delta^{18}O$ and $\delta^{2}H$ values which extended from the meteoric water line (Craig, 1961) towards $\delta^{18}O$ and $\delta^{2}H$ values characteristic of exchange with reservoir rocks. The intercept of this array with this line gives the $\delta^{18}O$ and $\delta^{2}H$ values of meteoric water at the time when it equilibrated with the clay minerals. Here we argue that this was during burial diagenesis.

2. Study area

We measured $\delta^{18}O$ and $\delta^{2}H$ values of muscovite (mu) and carbonate (carb) mineral separates from metamorphosed carbonate-bearing mudstone layers from Islay and the Garvellach Islands, western Scotland (Fig. 1). The studied sequence belongs to the Dalradian Supergroup and is comprised of the Garbh Eileach and Port Askaig Tillite Formations on the Garvellachs, and the Lossit Limestone, Port Askaig Tillite and Bonahaven Dolomite Formations on Islay (Fig. 1). The Garbh Eileach Formation which underlies the Port Askaig Tillite Formation on the Garvellachs is missing on Islay where the Port Askaig Tillite Formation overlies the older Lossit Limestone Formation. Both

formations contain shallow marine facies, including stromatolitic and dolomite horizons, interbedded with sandstone and limestones with variable siliciclastic mud content. The limestones contain ooid horizons indicative of a warm climate and, in the youngest beds, dolostones contain gypsum pseudomorphs indicative of arid conditions (Fairchild et al., 2018). A negative carbon isotope ($\delta^{13}C$) anomaly is preserved near the top of the Garbh Eileach Formation (Fairchild et al., 2018). This formation is overlain by the ~1-km-thick Port Askaig Tillite Formation which comprises sections of inferred glacial origin (Thomson 1871; Spencer, 1971; Fairchild et al., 2018; Ali et al., 2018). Forty-seven diamictite horizons are interlayered with sandstones, mudstones and (sometimes stromatolitic) dolostones (Spencer, 1971), from which 28 glacial advances and retreats are inferred (Ali et al., 2018). Most diamictites are massive and lack sedimentary layering. However, a few examples of finely layered marine or lacustrine sediments with dropstones have been reported (Spencer, 1971). Frost-shattered clasts and polygonal sandstone wedges atop several diamictite horizons as well as gypsum pseudomorphs in dolostone between some diamictites provide evidence of subaerial exposure and arid conditions between some glacial advances (Spencer, 1971; Fairchild et al., 2018; Ali et al., 2018), whereas cross-bedding, conglomerate beds and stromatolitic dolostones between other diamictites provide evidence of tidal or marine conditions between other glacial advances (Spencer, 1971). The age of the formation itself is not well constrained radiometrically. However, chemostratigraphic considerations strongly support a correlation with Sturtian glaciation (Prave et al., 2009; Ali et al., 2018). This formation is conformably overlain by mixed carbonate-siliciclastic sediments of the 250m thick Bonahaven Dolomite Formation (Spencer and Spencer, 1972). This formation is similar to a cap carbonate in that it preserves an extreme negative $\delta^{13}C$ excursion and overlies a glacial succession, but it differs in that no sharp boundary is observed with the underlying diamictites, the facies are peritidal (Fairchild, 1980), and its high content of clastic material is atypical for cap carbonates (Prave et al., 2009). The formation comprises stromatolitic dolostones, sandstones and variably dolomitic mudstones. The studied sequence is overlain by the Jura Quartzite Formation. This is an up-to-5-km-thick sequence of cross-bedded and pebbly quartzites which were deposited on a tidal shelf (Anderton, 1976) before the onset of late Cryogenian (Marinoan) glaciation (Prave et al., 2009) at 650–639 Ma (Hoffman et al., 2017).

This sequence of sedimentary rocks was deposited in fault-bounded basins during crustal extension prior to the opening of the Iapetus Ocean (Anderton, 1985) at low latitudes (Li et al., 2013). Sediment accumulation was rapid because of fast subsidence (Stephenson et al., 2013) associated with crustal extension. We thus infer that burial diagenesis occurred shortly after deposition, i.e. before the end of the Cryogenian Period.

During the mid-Ordovician Grampian Orogeny, major fold systems were formed (Tanner et al., 2013). One of these is a set of mostly NE-plunging *en echelon* anticlinal folds collectively referred to as the Islay Anticline (Fig. 1). Metamorphism at this time was at greenschist facies conditions with peak temperatures ranging from 400 to 500°C and maximum pressures of 1.0 ± 0.2 GPa (Skelton et al., 1995). The subsequent flow of metamorphic fluids affected parts of the study area, specifically zones of structural weakness, such as the axial region of the Islay Anticline (Skelton et al., 2015).

3. Methods

Samples of unweathered carbonate-bearing mudstones were collected from Lossit (L), Caol Ila (CI), Bunnahabhainn (BH) and along a section from Bolsa to Ruvaal (B-R) on Islay and from Eileach an Naoimh (EN), A' Chuli (AC) and Garbh Eileach (GE) which belong to the Garvellach Islands (Fig. 1, Table 1). The section from Bolsa to Ruvaal crosses the fold hinge of the Islay Anticline. Determination of stratigraphic and structural positions was based on previous work (Spencer, 1971; Skelton et al., 1995; Fairchild et al., 2018; Ali et al., 2018). Samples were used to make thin sections and powders for petrographic and isotopic analysis. Petrographic analysis of thin sections revealed that samples contained carbonates, quartz and muscovite. A few samples also contained small amounts of biotite, pyrite or graphite. Carbonate was removed from sample aliquots intended for δ^2H analysis by repeated washing with hydrochloric acid until the reaction ceased. Microscopic examination of these samples confirmed that they consisted of quartz and muscovite. In most cases, muscovite content was between 20 and 60 vol. %. Muscovite was concentrated by repeatedly shaking the sample on an inclined frosted glass plate. Quartz grains rolled freely down the plate leaving "stickier" muscovite flakes behind. The purity of the separate (>80 vol. %) was confirmed by microscopic examination.

Sample powders containing carbonates (calcite or dolomite, which were distinguished from one another by chemical analysis of sample powders using a handheld X-ray fluorescence analyser, see Table 1) were analysed for $\delta^{13}C$ and $\delta^{18}O$ at the Stable Isotope Laboratory (SIL) of the Department of Geological Sciences at Stockholm University (Table 1). Sample aliquots corresponding to 0.25 mg carbonate were reacted with excess of 100-percent phosphoric acid at 100°C for 1 hour before analysis of CO_2 using a Gasbench II connected to a MAT253 isotope ratio mass spectrometer, both from Thermo Scientific. Repeat analysis of NBS18, IAEA-CO-1 and IAEA-CO-8 standards and two controls gave standard deviations better than 0.1 ‰ for $\delta^{13}C$ and 0.15 ‰ for $\delta^{18}O$. Replicate analyses of randomly chosen samples ensured reproducibility. The reported $\delta^{18}O$ values were calculated according to the approach of Rosenbaum and Sheppard (1986) which takes into account the different temperature-dependent fractionation factors of calcite and dolomite when reacted with phosphoric

acid. Note that this was not accounted for by Skelton et al. (2015) which explains the slight shift between their results and those reported here (Fig. 3e). Normalization of results was performed using IAEA-CO-1 and NBS18 standards.

Acid-washed powders were analysed for δ^2H at the Scottish Universities Environmental Research Centre (SUERC) at the University of Glasgow (Table 1). Samples were heated to 120°C overnight under high vacuum to release labile volatiles after loading into thoroughly outgassed platinum crucibles. Samples were then gradually heated by radiofrequency induction in an evacuated quartz tube to >1200°C. The released water was then reduced to H_2 in a chromium furnace at 800°C according to the method of Donnelly et al. (2001), with the evolved gas measured quantitatively in a Hg manometer, then collected using a Toepler pump. The gas was subsequently analysed on a VG Optima mass spectrometer mass spectrometer. Replicate analyses of water standards (international standards V-SMOW and GISP, and internal standard Lt Std) gave a reproducibility of ±2 ‰. Replicate analyses of international mineral standard NBS-30 (biotite) gave reproducibility around ±3 ‰. The effect of acid washing on measured δ^2H values, determined by analysing samples before and after acid washing, was found to be negligible. Replicate analyses of randomly chosen samples ensured reproducibility.

Values of $\delta^{18}O$ for muscovite were calculated from $\delta^{18}O$ values for carbonate using fractionation factors for calcite-water (O'Neil et al., 1969), muscovite-water (O' Neil and Taylor, 1969) and dolomite-calcite (Sheppard and Schwarcz, 1970) at the metamorphic temperature (T) estimated by Skelton et al. (1995). We calculated respective fractionation factors (Δ) for calcite-muscovite and dolomite-muscovite of 1.7–1.9 and 2.0–2.5 at T = 400–500°C. Calculated $\delta^{18}O$ values were compared with measured values of $\delta^{18}O$ for muscovite separates from five samples, obtained as follows: O_2 was extracted from muscovite separates using a laser fluorination procedure, involving total sample reaction with excess ClF_3 using a CO_2 laser as a heat source (>1500°C) following the method of Sharp (1990). Oxygen was then converted to CO_2 by reaction with hot graphite, and analysed on-line by a VG Isotech SIRA II spectrometer. Reproducibility was around ±0.3‰ (1σ), based on repeat analyses of international and internal lab standards run during these analyses. Results are reported in standard notation ($\delta^{18}O$) as per mil (‰) deviations from the Standard Mean Ocean Water (V-SMOW) standard. A plot of measured $\delta^{18}O$ values for muscovite versus values calculated from $\delta^{18}O$ values for calcite (Fig. 4) shows a good linear relationship (R^2 = 0.95) close to (within ~1 ‰ of) 1:1. This confirms isotopic equilibrium between calcite and muscovite, implying that our calculated $\delta^{18}O$ values are valid.

4. Results

Isotopic data from metamorphosed carbonate-bearing mudstones in the study area form an elongated cluster on a δ^2H-$\delta^{18}O$ diagram with δ^2H_{mu} ranging from -89 to -47 ‰ and $\delta^{18}O_{mu}$ ranging from 10 to 24 ‰ (Fig. 2). These $\delta^{18}O$ and δ^2H values represent the time-integrated result of several processes each of which can cause isotopic modification since clay formation. These are post-depositional exchange with reservoir rocks (Sheppard, 1986), metamorphic volatilization (Valley, 1986) and exchange with metamorphic fluids (Bickle and McKenzie,1987). These processes will be considered sequentially in reverse order.

5. Exchange with metamorphic fluids

Metamorphic fluid flow in the study area was strongly channelled along fold hinges, particularly the Islay Anticline (Fig. 1), which acted as structural conduits for fluids escaping from below (Skelton et al., 1995; 2015). Fluid fluxes were sufficient to modify $\delta^{13}C$ values (Skelton et al., 2015) and therefore also $\delta^{18}O$ and δ^2H values, because fluid (compared with rocks) tends to contain more oxygen and hydrogen than carbon. Sections close to the Islay Anticline and affected by, and far from the Islay Anticline and unaffected by, metamorphic fluid flow can be seen on stratigraphic profiles of $\delta^{13}C$, $\delta^{18}O$ and δ^2H values (Fig. 3). The Garbh Eileach, Lossit Limestone and Port Askaig Tillite Formations are largely unaffected by metamorphic fluid flow. The Garbh Eileach Formation carbonates preserve a negative $\delta^{13}C$ anomaly with minimum $\delta^{13}C$ values of -6 ‰. In this formation, $\delta^{18}O$ values range from 20 to 25 ‰ and δ^2H values range from -65 to -55 ‰. In the Port Askaig Tillite Formation, $\delta^{13}C$, $\delta^{18}O$ and δ^2H values decrease up-sequence: $\delta^{13}C$ from ~0 to -5 ‰, $\delta^{18}O$ from 20-25 to ~13 ‰ and δ^2H from ~-60 to ~-70 ‰. The Bonahaven Dolomite Formation was sampled close to the axis of the Islay Anticline and the effects of metamorphic fluid flow can be seen. Unravelling these effects from the effects of stratigraphic position is made possible by repetition of parts of this formation by faulting (Fig. 1). In one section, Members 3 and 4 of this formation straddle the fold axis and are likely to have been affected by metamorphic fluid flow (Skelton et al., 2015). In the other section, members 3 and 4 are far (1-2 km) from the fold axis and are less likely to have been affected by metamorphic fluid flow. Member 3 preserves negative $\delta^{13}C$ values typical of cap carbonates (-8 to -3 ‰). These values are unaffected by metamorphic fluid flow along the fold axis (Fig. 3). This is, however, expected because the $\delta^{13}C$ value of metamorphic fluid (-6.1 ‰: Skelton et al., 2015) falls within this range. In contrast, member 4 preserves extremely positive $\delta^{13}C$ values and is strongly affected by metamorphic fluid flow: $\delta^{13}C$ ~10 ‰ far from the fold axis and $\delta^{13}C$ ~5 ‰ close to the

fold axis (Fig. 3). Both $\delta^{18}O$ and $\delta^{2}H$ values are also much lower close to the fold hinge: $\delta^{18}O$ by ~5 ‰ and $\delta^{2}H$ by ~40 ‰. This points to exchange with a metamorphic fluid which is isotopically light with respect to carbon, oxygen and hydrogen. It is likely that the source of this fluid was the underlying Ballygrant and Glenegadale Slate Formations (Fig. 1) because these consist of graphitic, formerly organic-rich mudstones (Sheppard, 1986). We conclude that metamorphic fluid flow along the axis of the Islay Anticline has modified stable isotope values, but this effect is spatially restricted to within <200 m of the fold axis (Fig. 3). Thus samples from this region were excluded from further analysis (Fig. 2).

6. Metamorphic volatilization

Metamorphic volatilization refers to the release of volatile species caused by metamorphic reactions. Release of H_2O (metamorphic dehydration) can cause fractionation of H and O isotopes. The isotopic shift ($\delta_{water} - \delta_{rock}$) for either H or O caused by dehydration, assuming Rayleigh isotope fractionation is given by:

$$\delta_{water} - \delta_{rock} = 1000\left(F^{(\alpha-1)} - 1\right) \quad (1)$$

where *F* is the mole fraction of the element of interest (H or O) remaining in the rock after dehydration and α is the water-rock fractionation factor. The effect of dehydration on $\delta^{18}O$ values is negligible and can therefore be ignored (Valley, 1986). This is because a maximum of ~5 wt. % H_2O (which contains 89 wt. % O) can be released by metamorphic dehydration whereas rocks contain ~50 wt. % O, which gives $F \geq 0.9$. In contrast, because rocks contain little or no H, values of *F* for H can range down to zero and $\delta^{2}H$ values can therefore be strongly affected by dehydration (Valley, 1986). Here, we assume that muscovite was produced by metamorphic dehydration of illite. This is motivated by the fact that illite is the predominant clay mineral at diagenetic conditions in mudstones (Huggett, 2005). For complete replacement of illite (which contains 1.38 wt. % H) by muscovite (which contains 0.46 wt. % H), *F* = 0.33. The value of α, which is insensitive to temperature (Sheppard and Gilg, 1986), is 1.025 ± 0.005 for water-illite (O' Neil and Kharaka, 1976) and ranges from 1.030 at 400°C to 1.018 at 500°C for water-muscovite (Suzuoki and Epstein, 1976). From equation (1) with *F* = 0.33 and α ranging from 1.018 to 1.030, $\delta_{water} - \delta_{rock}$ ranges from -19.6 to -32.4 ‰. This is the $\delta^{2}H$ depletion for replacement of illite by muscovite during metamorphism. Subtraction of this depletion yields calculated $\delta^{18}O$ and $\delta^{2}H$ values for illite before metamorphism (Fig. 2).

7. Meteoric water

The $\delta^{18}O$ and $\delta^{2}H$ values of pore water in equilibrium with illite at diagenetic conditions can be calculated from water-illite isotope fractionation factors. These are 10–15 ‰ for oxygen and 20–30 ‰ for hydrogen (Sheppard and Gilg, 1986) for the temperature range of illite authigenesis (80–120°C Glasmann et al., 1989; Eberl, 1993). Subtracting these factors reveals a $\delta^{18}O$ and $\delta^{2}H$ array for pore waters which extends from the meteoric water line, MWL ($\delta^{2}H = 8\ \delta^{18}O + 10$: Craig, 1961) towards higher of $\delta^{18}O$ and $\delta^{2}H$ values (Fig. 2). This trend, which is typical for pore waters from sedimentary basins, probably reflects exchange between meteoric water and reservoir rocks (Clayton et al., 1966). Its intercept with the meteoric water line falls within the 2σ ranges -34 ± 10 ‰ = -1 to -4 ‰ and $\delta^{2}H$ = 0 to -23 ‰. This is the inferred isotopic composition of meteoric water in equilibrium with illite at 80–120°C. This was probably reached at an approximate burial depth of 3–4 km (by analogy with the present day Gulf of Mexico: Eberl, 1993).

8. Implications

The $\delta^{18}O$ and $\delta^{2}H$ ranges we calculated for meteoric water are similar to present day values at the latitude range (30-35°S) where the sediments in our study area were both deposited and buried (Dansgaard, 1964; Jouzel et al., 1994). Our $\delta^{18}O$ range differs from values attributed by previous workers to Snowball Earth and its immediate aftermath. These range from -11 ± 4 ‰ to -34 ± 10 ‰ (Fairchild et al., 2016; Kennedy et al., 2008; Peng et al., 2013; Herwartz et al., 2015) and are similar to meltwater from subpolar to polar regions (Robinson et al., 2009; Schotterer et al., 1997). We infer that the less negative values we calculated reflect a climate similar to present day (Ice Age) conditions at the time when burial diagenesis occurred. This was most likely after Sturtian glaciation but, we assume, before the end of the Cryogenian Period because of the rapidity of sediment accumulation at that time (Stephenson et al., 2013). We thereby infer that our $\delta^{18}O$ and $\delta^{2}H$ ranges define a “baseline” for the Cryogenian Period, whereas previously reported more negative values represent Snowball Earth episodes. The baseline we defined might be overrepresented in the geological record because sediment accumulation was heavily biased towards (short-lived) warmer episodes at the end of Snowball Earth episodes, which were themselves characterized by little or no sediment accumulation (Hoffman et al., 2017).

Overall, our findings support the idea that a Snowball Earth episode is represented by a hiatus in the geological record, whereas glacial rocks were deposited in its aftermath or later on (cf. Hoffman et al., 2017). This idea is further supported by sedimentological evidence for multiple glacial advances and retreats in our study area (Spencer, 1971; Ali et al., 2018) and other Cryogenian deposits (e.g. Fairchild et al., 2016).

Finally, we note that the approach used here could be used to "remove" the effects of post-depositional exchange with reservoir rocks, metamorphic volatilization and/or exchange with metamorphic fluids in other isotopic studies of Precambrian rocks.

9. Sensitivity analysis

The validity of our calculated $\delta^{18}O$ and $\delta^{2}H$ values for Cryogenian meteoric water relies on several of assumptions, each of which can be flawed. It is therefore necessary to assess how sensitive our calculated values are to each assumption.

We assumed that the effect of metamorphic fluid flow was spatially restricted. This assumption is supported by $\delta^{18}O$ data (Skelton et al., 2015). Metamorphic fluid flow caused a shift towards more negative $\delta^{18}O$ and $\delta^{2}H$ values because of exchange with organic shales upstream of the studied sequence (Skelton et al., 2015). If this was more extensive than assumed, calculated values of $\delta^{18}O$ and $\delta^{2}H$ before metamorphic fluid flow would be less negative.

We assumed that muscovite in our samples was produced by metamorphism of illite, because it is the predominant clay mineral at diagenetic conditions in mudstones (Huggett, 2005). Values of α range from 1.024 at 100°C to 1.013 at 400°C for water-kaolinite and 1.015 ± 0.005 for water-montmorillonite (Glasmann et al., 1989). Also F = 0.29 for kaolinite and 0.11 for montmorillonite. With these values of α and F, the calculated minimum values for $\delta_{water} - \delta_{rock}$ are -15.3 to -36.1 ‰ for kaolinite and -21.6 to -63.4 ‰ for montmorillonite. This would extend our $\delta^{18}O$ and $\delta^{2}H$ ranges, but only towards less negative values.

We assumed that meteoric water and clay equilibrated at diagenetic conditions (80–120°C). If this assumption were flawed and clay was formed by weathering, equilibration would have occurred at lower temperature (Lawrence and Taylor, 1972). For the temperature range 0–25°C, water-illite isotope fractionation factors would be ~13 ‰ higher for oxygen (Sheppard and Gilg, 1986). Meteoric water compositions would then extend above MWL on Fig. 2, predicting deuterium excesses from 10

to 110 ‰. These are unreasonably high, predicting negative relative humidities (Pfahl and Wernli, 2008).

We assumed that illite formed at a burial depth of 3–4 km by analogy with the Gulf of Mexico (Eberl, 1993). We infer that this burial depth was reached in our study area before the onset of late Cryogenian (Marinoan) glaciation based on lithostratigraphy (Stephenson et al., 1993; Prave et al., 2009). If illite formed at 80–120°C (Glasman et al., 1989), a geothermal gradient of approximately 30°C/km is implied. Our conclusion still holds for geothermal gradients ranging from 20 to 60°C/km. If the geothermal gradient was even lower, a burial depth greater than the thickness of Cryogenian sediments on top of the studied sequence would be required to reach temperatures required for illite authigenesis. However, we point out that extensive spilitisation of basaltic sills affected our study area (Graham, 1976) at 595 ± 4 Ma (Halliday et al., 1989), necessitating temperatures far higher than are required for illite authigenesis. We thus conclude that in the unlikely event that our results relate to a time after the end of the Cryogenian Period, this must have been in the early Ediacaran Period and prior to the Gaskiers glaciation at 580 Ma (Pu et al., 2016).

In summary, failure of any of the aforementioned assumptions can either be ruled out or has only limited effect on the conclusions of our study. Finally, we note that the validity of the approach we have used is supported by the fact that the $\delta^{18}O$ and $\delta^{2}H$ array we obtained for pore water extends from the meteoric water line in a manner that is expected from sedimentary basins.

Acknowledgements

The Swedish Research Council and the Bolin Centre for Climate Research are acknowledged for financial support. The late Dan Zetterberg is acknowledged for assisting with rock preparation.

References

Ali, D.O., Spencer, A.M., Fairchild, I.J., Chew, K.J., Anderton, R., Levell, B.K., Hambrey, M.J., Dove, D., Le Heron, D.P. 2018. Indicators of relative completeness of the glacial record of the Port Askaig Formation, Garvellach Islands, Scotland. Precambrian Research, doi: 10.1016/j.precamres.2017.12.005.

Anderton, R. 1976. Tidal-shelf sedimentation: an example from the Scottish Dalradian. Sedimentology 23, 429–458.

Anderton, R. 1985. Sedimentation and tectonics in the Scottish Dalradian. Scottish Journal of Geology 21, 407–436.

Bickle, M. J., McKenzie, D. 1987. The transport of heat and matter by fluids during metamorphism. Contributions to Mineralogy and Petrology 95, 384–392.

Bindeman, I.N., Serevryakov, N.S. 2011. Geology, Petrology and O and H isotope geochemistry of remarkably ^{18}O depleted Paleoproterozoic rocks of the Belomorian Belt, Karelia, Russia, attributed to global glaciation 2.4 Ga. Earth and Planetary Science Letters 306, 163–174.

Clayton, R.N., Friedman, I., Graf, D.L., Mayeda, T.K., Meents, W.F., Shimp, N.F. 1966. The origin of saline formation waters. Journal of Geophysical Research 71, 3869–3882.

Craig, H. 1961. Isotopic variation in meteoric waters. Science 133, 1702–1703.

Dansgaard, W. 1964. Stable isotopes in precipitation. Tellus 16, 436–468.

Donnelly, T., Waldron, S., Tait, A., Dougans, J., Bearhop, S. 2001. Hydrogen isotope analysis of natural abundance and deuterium-enriched waters by reduction over chromium on-line to a dynamic dual inlet isotope-ratio mass spectrometer. Rapid Communications in Mass Spectrometry 15, 1297–1303.

Eberl, D.D. 1993. Three zones for illite formation during burial diagenesis and metamorphism. Clays and Clay Minerals 41, 26–37.

Fairchild, I.J. 1980. Sedimentation and origin of a Late Precambrian 'dolomite' from Scotland. Journal of Sediment Petrology 50, 423–466.

Fairchild, I.J., Spencer, A.M., Ali, D.O., Anderson, R.P., Anderton, R., Boomer, I., Dove, D., Evans, J.D., Hambrey, M.J., Howe, J., Sawaki, Y., Wang, Z., Shields, G., Skelton, A., Tucker, M.E., Zhou, Y. 2018. Tonian-Cryogenian boundary sections of Argyll, Scotland. Precambrian Research, doi: 10.1016/j.precamres.2017.09.020.

Fairchild, I.J, Fleming, E.J., Bao, H., Benn, D.I., Boomer, I., Dublyansky, Y.V., Halverson, G.P., Hambrey, M.J., Hendy, C., McMillan, E.A., Spötl, C., Stevenson, C.T.E., Wynn, P.M. 2016. Continental carbonate facies of a Neoproterozoic panglaciation, north-east Svalbard. Sedimentology 63, 443– 497.

Fallick, A. E., Macaulay, C. I., Haszeldine, R. S. 1993. Implications of linearly correlated oxygen and hydrogen isotopic compositions for kaolinite and illite in the Magnus Sandstone, North Sea. Clays and Clay Minerals 41, 184–190.

Glasmann, J.R., Lundegard, P.D., Clark, R.A., Penny, B.K., Collins, I.D. 1989. Geochemical evidence for the history of diagenesis and fluid migration: Brent Sandstone, Heather Field, North Sea. Clay Minerals 24, 255–284.

Graham, C.M. 1976. Petrochemistry and tectonic significance of Dalradian metabasaltic rocks of the SW. Scottish Highlands. Journal of the Geological Society 132, 61–84.

Halliday, A. N., Graham, C. M., Aftalion, M., Dymoke, P., 1989. The depositional age of the Dalradian Supergroup, U–Pb and Sm–Nd isotopic studies of the Tayvallich volcanics, Scotland. Journal of the Geological Society 146, 3–6.

Herwartz, D., Packa, A., Krylovb, D., Xiaoc, Y., Muehlenbachsd, K., Senguptaa, S., Di Roccoa, T. 2015. Revealing the climate of snowball Earth from $\Delta^{17}O$ systematics of hydrothermal rocks. PNAS 112, 5337–5341.

Hoffman, P.F., Abbot, D.S., Ashkenazy, Y., Benn, D.I., Brocks, J.J., Cohen, P.A., Cox, G. M., Creveling, J.R., Donnadieu, Y., Erwin, D.H., Fairchild, I.J., Ferreira, D., Goodman, J.C., Halverson, G.P., Jansen, M.F., Le Hir, G., Love, G.D., Macdonald, F.A., Maloof, A.C., Partin, C.A., Ramstein, G., Rose, B.E.J., Rose, C.V., Sadler, P.M., Tziperman, E., Voigt, A., Warren, S.G. 2017. Snowball Earth climate dynamics and Cryogenian geology-geobiology. Science Advances e1600983.

Huggett, J.M. 2005. Clays and their Diagenesis. In: Selley, R.C., Cocks, L.R.M., Plimer, I.R. (Eds.), Encyclopedia of Geology 5. Elsevier, Amsterdam, pp. 61–69.

Jouzel, J., Koster, R.D., Suozzo, R.J., Russell, G.L. 1994. Stable water isotope behavior during the last glacial maximum: A general circulation model analysis. Journal of Geophysical Research 99, 25791–25801.

Kennedy, M.J., Mrofka, D., von der Borch, C.C. 2008. Snowball earth termination by destabilization of equatorial permafrost methane clathrate. Nature 453, 642–645.

Lawrence, J.R., Taylor, H.P. 1972. Hydrogen and oxygen isotope systematics in weathering profiles. Geochimica et Cosmochimica Acta 36, 1377–1393.

Li., Z.-X., Evans, D.A.D., Halverson, G.D. 2013. Neoproterozoic glaciations in a revised global palaeogeography from the breakup of Rodinia to the assembly of Gondwanaland. Sedimentary Geology 294, 219–232.

O'Neil, J.R., Clayton, R.N., Mayeda, T.K. 1969. Oxygen isotope fractionation in divalent metal carbonates. The Journal of Chemical Physics 51, 5547.

O'Neil, J.R., Kharaka, Y.K. 1976. Hydrogen and oxygen isotope exchange reactions between clay minerals and water. Geochimica et Cosmochimica Acta 40, 241–246.

O'Neil, J.R., Taylor, H.P. 1969. Oxygen Isotope Equilibrium between Muscovite and Water. Journal of Geophysical Research 74, 6012–6022.

Peng, Y., Bao, H., Zhou, C., Yuan, X., Luo, T. 2013. Oxygen isotope composition of meltwater from a Neoproterozoic glaciation in South China. Geology 41, 367–370.

Pu, J.P., Bowring, S.A., Ramezani, J., Myrow, P., Raub, T.D., Landing, E., Mills, A., Hodgin, E., Macdonald, F.A. 2016. Dodging snowballs: Geochronology of the Gaskiers glaciation and the first appearance of the Ediacaran biota. Geology 44; p. 955–958.

Pfahl, S., Wernli, H. 2008. Air parcel trajectory analysis of stable isotopes in water vapor in the eastern Mediterranean. Journal of Geophysical Research 113, D20104.

Prave, A. R., Fallick, A. E., Thomas, C. W., Graham, C. M. 2009. A composite C-isotope profile for the Neoproterozoic Dalradian Supergroup of Scotland and Ireland. Journal of the Geological Society of London 166, 845–857.

Robinson, Z.P., Fairchild, I.J., Arrowsmith, C. 2009. Stable isotope tracers of shallow groundwater recharge dynamics and mixing within an Icelandic sandur, Skeiðarársandur. Hydrology in Mountain Regions: observations. In: Processes and Dynamics (Proceedings of Symposium HS1003 at IUGG2007, Perugia, July 2007). International Association of Hydrological Science Publications 326, 119–125.

Rosenbaum, J., Sheppard, S. M. F. 1986. An isotopic study of siderites, dolomites and ankerites at high temperatures. Geochimica et Cosmochimica Acta 50, 1147–1150.

Schotterer, U., Frohlich, K., Gaggeler, H.W., Sandjordj, S., Stichler, W. 1997. Isotope records from Mongolian and alpine ice cores as climate indicators. Climatic Change 36, 519–530.

Sharp, Z.D. 1990. A laser-based microanalytical method for the in situ determination of oxygen isotope ratios in silicates and oxides. Geochimica Cosmochimica Acta 54, 1353–1357.

Sheppard, S.M.F. 1986. Characterization and isotopic variations in natural waters. In: Valley, J.W., Taylor Jr., H.P., O'Neil, J.R. (Eds.), Stable isotopes in high temperature geological processes. Reviews in Mineralogy 16, Mineralogical Society of America, Virginia, pp. 165–183.

Sheppard, S. M. F., Gilg 1986. H. A. Stable isotope geochemistry of clay minerals. Clay Minerals 31, 1–24.

Sheppard, S.M.F., Schwarcz, H.P. 1970. Fractionation of carbon and oxygen isotopes and magnesium between metamorphic calcite and dolomite. Contributions to Mineralogy and Petrology 26, 161–198.

Skelton, A., Lewerentz, A., Kleine, B., Webster, D., Pitcairn, I. 2015. Structural Channelling of Metamorphic Fluids on Islay, Scotland: Implications for Paleoclimatic Reconstruction. Journal of Petrology 56, 2145–2172.

Skelton, A. D. L., Graham, C. M., Bickle, M. J. 1995. Lithological and structural controls on regional 3-D fluid flow patterns during greenschist facies metamorphism of the Dalradian of the SW Scottish Highlands. Journal of Petrology 36, 563–586.

Spencer, A. M. 1971. Late Pre-Cambrian glaciation in Scotland. Memoir of the Geological Society of London 6, 112 pp.

Spencer, A. M., Spencer, M. O. 1972. The Late Precambrian / Lower Cambrian Bonahaven Dolomite of Islay and its stromatolites. Scottish Journal of Geology 8, 269–282.

Stephenson, D., Mendum, J.R., Fettes, D.J., Leslie, A.G. 2013. The Dalradian rocks of Scotland: an introduction. Proceedings of the Geologists' Association 124, 3–82.

Suzuoki, T., Epstein, S. 1976. Hydrogen isotope fractionation between OH-bearing minerals and water. Geochimica et Cosmochimica Acta 40, 1229–1240.

Tanner, G., Bendall, C.A., Pickett, E.A., Roberts, J.L., Treagus, J.E., Stephenson, D. 2013. The Dalradian rocks of the south-west Grampian Highlands of Scotland. Proceedings of the Geologists' Association 124, 83–147.

Thomson, J. 1871. On the stratified rocks of Islay. In: Report of the British Association for the Advancement of Science, 41st. Meeting, Edinburgh, John Murray, London, pp. 110–111.

Valley, J.W. 1986. Stable isotope geochemistry of metamorphic rocks. In: Valley, J.W., Taylor Jr., H.P., O'Neil, J.R. (Eds.), Stable isotopes in high temperature geological processes. Reviews in Mineralogy 16, Mineralogical Society of America, Virginia, pp. 445–486.

FIGURE CAPTIONS

Fig. 1. Geological map and stratigraphic column of Islay and the Garvellach Islands. The Lossit/Garbh Eileach, Port Askaig Tillite and Bonahaven Dolomite Formations are shown on the stratigraphic column. Samples were collected from the following areas: Lossit (L), Caol Ila (CI), Bunnahabhainn (BH) and along a section from Bolsa to Ruvaal (B-R) on Islay and Eileach an Naoimh (EN), A' Chuli (AC) and Garbh Eileach (GE) on the Garvellach Islands (see Table 1 for sample locations). The *en echelon* segments of the Islay Anticline are shown.

Fig. 2. δ^2H – $\delta^{18}O$ plot showing measured δ^2H and calculated $\delta^{18}O$ values for muscovite (green symbols), calculated δ^2H and $\delta^{18}O$ values for illite before metamorphism (red symbols), and calculated δ^2H and $\delta^{18}O$ values for pore water at the time of equilibration with illite (blue symbols). Square, circular and triangular symbols represent samples from the Lossit/Garbh Eileach, Port Askaig Tillite and Bonahaven Dolomite Formations, respectively. If not shown, analytical errors are smaller than the symbols. The symbols which lack colour are from within 200 m of the axial plane of the Islay Anticline. These are affected by metamorphic fluid flow and excluded from further analysis. The solid blue line is the meteoric water line (MWL: Craig, 1961). The blue lines mark the 2 standard deviation error envelope for the best fit linear trend through calculated pore water δ^2H and $\delta^{18}O$ values.

Fig. 3. Stratigraphic and structural plots of $\delta^{13}C_{carb}$, $\delta^{18}O_{carb}$ and δ^2H_{mu} values. These are plotted against approximate stratigraphic position (Spencer, 1971; Fairchild et al., 2018; Ali et al., 2018) (a-c) and on structural plots (d-f) as a function of distance from the Islay Anticline (red line) for the Bolsa to Ruvaal section (B-R on Fig. 1). Green symbols are from this study. Open symbols show previously published values from the Lossit/Garbh Eileach Formation (Prave et al., 2009) and the Bonahaven Dolomite Formation (Skelton et al., 2015). Blue shading and square symbols represent the Lossit/Garbh Eileach Formation. Brown shading and circular symbols represent the Port Askaig Tillite Formation. Purple shading and triangular symbols represent the Bonahaven Dolomite Formation. Repetition of members 3 and 4 of the Bonahaven Dolomite Formation by folding and faulting is seen on the structural plots (d-f).

Fig. 4. Measured $\delta^{18}O_{mu}$ values plotted against $\delta^{18}O_{mu}$* values which are calculated from $\delta^{18}O_{carb}$ using fractionation factors. The best fit linear regression (dashed line, $R^2 = 0.95$) is compared with the 1:1 line (solid line).

Table 1

Sample	Mineralogy	Locality	Latitude	Longitude	Formation	Member	$\delta^{13}C_{carb}$	$\delta^{18}O_{carb}$	$\delta^{18}O_{mu}$	$\delta^{18}O_{mu}$*	$\delta^{18}O_{H2O}$*	$\delta^{2}H_{mu}$	$\delta^{2}H_{illite}$*	$\delta^{2}H_{H2O}$*
PS-16-01*	mu, q, dol	B-R	55° 55.499' N	6° 11.332' W	BDF	4	4.9	13.6		11.4		-64.1		
PS-16-02*	mu, q, dol	B-R	55° 55.500' N	6° 11.331' W	BDF	4	5.4	13.8		11.6		-82.2		
PS-16-10*	mu, q, dol	B-R	55° 55.489' N	6° 11.184' W	BDF	4	6.2	14.4		12.2		-88.6		
PS-16-11	mu, q, dol	B-R	55° 55.542' N	6° 10.769' W	BDF	3	-5.6	17.3		15.1	2.6	-51.5	-25.5	-0.5
DD-16-04	mu, q, dol	B-R	55° 56.500' N	6° 09.425' W	BDF	3	-6.4	17.0		14.8	2.3	-57.2	-31.2	-6.2
PS-16-12	mu, q, cc	B-R	55° 55.539' N	6° 10.644' W	BDF	3	-7.1	17.3		15.6	3.1	-46.8	-20.8	4.2
DD-16-06	mu, q, dol	B-R	55° 56.200' N	6° 09.072' W	BDF	3	-6.9	16.9		14.7	2.2	-57.7	-31.7	-6.7
BH-16-03b	mu, q, cc	BH	55° 52.762' N	6° 07.177' W	BDF	1	-3.3	18.6		16.8	4.3	-67.4	-41.4	-16.4
BH-16-03	mu, q, cc	BH	55° 52.763' N	6° 07.168' W	BDF	1	-3.4	17.3		15.5	3.0	-60.6	-34.6	-9.6
BH-16-02	mu, q, cc	BH	55° 52.750' N	6° 07.156' W	BDF	1	-2.8	20.2		18.4	5.9	-64.7	-38.7	-13.7
CI-16-02	mu, q	CI	55° 51.431' N	6° 06.555' W	BDF	1						-67.8	-41.8	-16.8
CI-16-01	mu, bi, q	CI	55° 51.375' N	6° 06.570' W	BDF	1						-69.8	-43.8	-18.8
BH-16-01	mu, q, cc	BH	55° 52.704' N	6° 07.118' W	BDF	1	-7.7	13.0		11.2	-1.3	-65.8	-39.8	-14.8
CI-16-03	mu, q, dol	CI	55° 51.460' N	6° 06.531' W	PATF	5	-4.0	13.9	12.2	11.7	-0.8	-61.9	-35.9	-10.9
CL-16-03	mu, q, dol	L	55° 49.353' N	6° 06.695' W	PATF	3	-4.5	12.7		10.5	-2.0	-64.2	-38.2	-13.2
GE-16-d32	mu, q, dol	GE	56° 14.579' N	5° 45.236' W	PATF	2	-2.2	13.5		11.3	-1.2	-70.0	-44.0	-19.0
GE-16-00	mu, q, dol	GE	56° 14.332' N	5° 46.645' W	PATF	2	-1.5	16.5	16.4	14.2	1.7	-60.7	-34.7	-9.7
AC-16-12	mu, q, dol	AC	56° 13.988' N	5° 47.370' W	PATF	2	-1.6	18.3		16.1	3.6	-67.2	-41.2	-16.2
LL-16-a	mu, q, cc	L	55° 48.520' N	6° 07.553' W	PATF	2	-1.3	17.8		16.0	3.5	-61.0	-35.0	-10.0
LL-16-e	mu, q, dol	L	55° 48.435' N	6° 07.823' W	PATF	2	0.0	22.2		20.0	7.5	-72.9	-46.9	-21.9
EN-16-02	mu, q, dol	EN	56° 13.017' N	5° 49.900' W	PATF	1	1.4	24.5	24.0	22.3	9.8	-62.3	-36.3	-11.3
AC-16-06	mu, q, cc	AC	56° 14.264' N	5° 46.847' W	PATF	1	-0.4	22.3		20.6	8.1	-63.6	-37.6	-12.6

LL-16-d	mu, q, dol	L	55° 48.467' N	6° 07.698' W	PATF	1	1.9	25.7		23.5	11.0	-55.8	-29.8	-4.8
GE-16-d11	mu, q, dol	GE	56° 14.850' N	5° 45.019' W	PATF	1	-1.0	21.2		19.0	6.5	-63.2	-37.2	-12.2
GE-16-d7	mu, q, dol	GE	56° 14.889' N	5° 45.042' W	PATF	1	-2.4	20.6		18.4	5.9	-59.2	-33.2	-8.2
GE-16-d1	mu, q, dol	GE	56° 14.941' N	5° 45.086' W	PATF	1	-0.2	22.7		20.5	8.0	-58.0	-32.0	-7.0
GE-16-45	mu, q, dol	GE	56° 14.947' N	5° 45.113' W	GEF		0.2	23.2		21.0	8.5	-55.4	-29.4	-4.4
GE-16-31	mu, q, dol	GE	56° 14.956' N	5° 45.140' W	GEF		-1.6	21.8		19.6	7.1	-59.7	-33.7	-8.7
GE-16-23	mu, q, dol	GE	56° 14.966' N	5° 45.158' W	GEF		-5.0	21.8		19.5	7.0	-56.3	-30.3	-5.3
GE-16-08	mu, q, dol	GE	56° 14.979' N	5° 45.280' W	GEF		-5.7	21.4	21.1	19.2	6.7	-64.9	-38.9	-13.9
LL-16-g	mu, q, cc	L	55° 48.412' N	6° 07.732' W	LLF		1.3	18.3	16.2	16.6	4.1	-58.6	-32.6	-7.6
LL-16-h	mu, q	L	55° 48.383' N	6° 07.655' W	LLF							-62.3	-36.3	-11.3

This table show sample names, mineralogy, locality, latitude and longitude, Formation and Member, measured values of $\delta^{13}C_{carb}$, $\delta^{18}O_{carb}$, $\delta^{18}O_{mu}$ and $\delta^{2}H_{mu}$, and calculated values of $\delta^{18}O_{mu}$*, $\delta^{18}O_{H2O}$*, $\delta^{2}H_{illite}$* and $\delta^{2}H_{H2O}$*. Values are reported per mil. (‰) relative to Vienna Pee Dee Belemnite (VPDB) for carbon isotopes and Vienna Standard Mean Ocean Water (VSMOW) for oxygen and hydrogen isotopes. Sample names marked with an asterisk (*) were collected within 200 m of the axial plane of the Islay Anticline and are consequently affected by metamorphic fluid flow. For this reason, values of $^{18}O_{mu}$*, $\delta^{18}O_{H2O}$*, $\delta^{2}H_{illite}$* and $\delta^{2}H_{H2O}$* were not calculated for these samples. Muscovite, quartz, dolomite and calcite are abbreviated mu, q, dol and cc, respectively. Localities: Bolsa-Rhuvaal, Bunnahabhainn, Caol Ila and Lossit (from Islay) and Garbh Eileach, A' Chuli, and Eileach an Naoimh (from the Garvellachs) are abbreviated B-R, BH, CI, L, GE, AC and EN. The subscripts "carb" and "mu" refer to carbonate (dolomite or calcite) and muscovite, respectively. Formations: Bonahaven Dolomite Formation, Port Askaig Tillite Formation, Garbh Eileach Formation and Lossit Limestone Formation are abbreviated BDF, PATF, GEF and LLF. The Garbh Eileach Formation was previously considered part of the Lossit Limestone Formation, but was redefined by Fairchild et al. (2018).

The $\delta^{18}O_{mu}$* values were calculated from $\delta^{18}O_{carb}$ by subtracting a fractionation factor (Δ) of 1.8 ‰ for samples containing calcite and 2.2 ‰ for samples containing dolomite. The value of $\Delta_{cc\text{-}mu}$ was calculated by combining values of $\Delta_{cc\text{-}H2O}$ and $\Delta_{mu\text{-}H2O}$ from O'Neil et al. (1969) and O'Neil & Taylor (1969), respectively, calculated at 450˚C. The value of $\Delta_{dol\text{-}mu}$ was calculated by combining the value of $\Delta_{cc\text{-}mu}$ with $\Delta_{dol\text{-}cc}$ from Sheppard & Schwarcz (1970) at 450˚C. These values were compared with measured values of $\delta^{18}O_{mu}$ for five samples

The $\delta^{2}H_{illite}$* values were calculated from $\delta^{2}H_{mu}$ by subtracting a calculated isotopic shift for metamorphic volatilization ($\delta_{water} - \delta_{rock}$) of -26.0 ± 6.4 ‰. This value was calculated from the equation: $\delta_{water} - \delta_{rock} = 1000\left(F^{(\alpha-1)} - 1\right)$, from Valley (1986)[11], which assumes Rayleigh

fraction and where *F* is the mole fraction of hydrogen remaining in the rock after dehydration and α is the water-rock fractionation factor. The value of *F* was set to 0.33 for complete replacement of illite (which contains 1.38 wt. % H) by muscovite (which contains 0.46 wt. % H) and the value of α was set to 1.018–1.030 which corresponds to the full range of values for illite and muscovite in the respective temperature ranges 100–400˚C from O'Neil & Kharaka (1976) and 400–500˚C from Suzuoki & Epstein (1976).

The δ^2H_{H2O}* values were calculated from δ^2H_{illite}* by subtracting a fractionation factor of 25 ± 5 ‰ from Sheppard & Gilg (1986).

The effect of dehydration on $\delta^{18}O$ values was assumed to be negligible and was therefore ignored (Valley, 1986). The $\delta^{18}O_{H2O}$* values were thus calculated directly from $\delta^{18}O_{mu}$* by subtracting a fractionation factor of 12.5 ± 2.5 ‰ from Sheppard & Gilg (1986).

Highlights

- Baseline $\delta^{18}O$ and $\delta^{2}H$ of Cryogenian meteoric water are similar to the present day.
- Snowball Earth episodes are associated with negative excursions from this baseline.
- Effects of post-depositional exchange can be removed from $\delta^{18}O$ and $\delta^{2}H$ records.

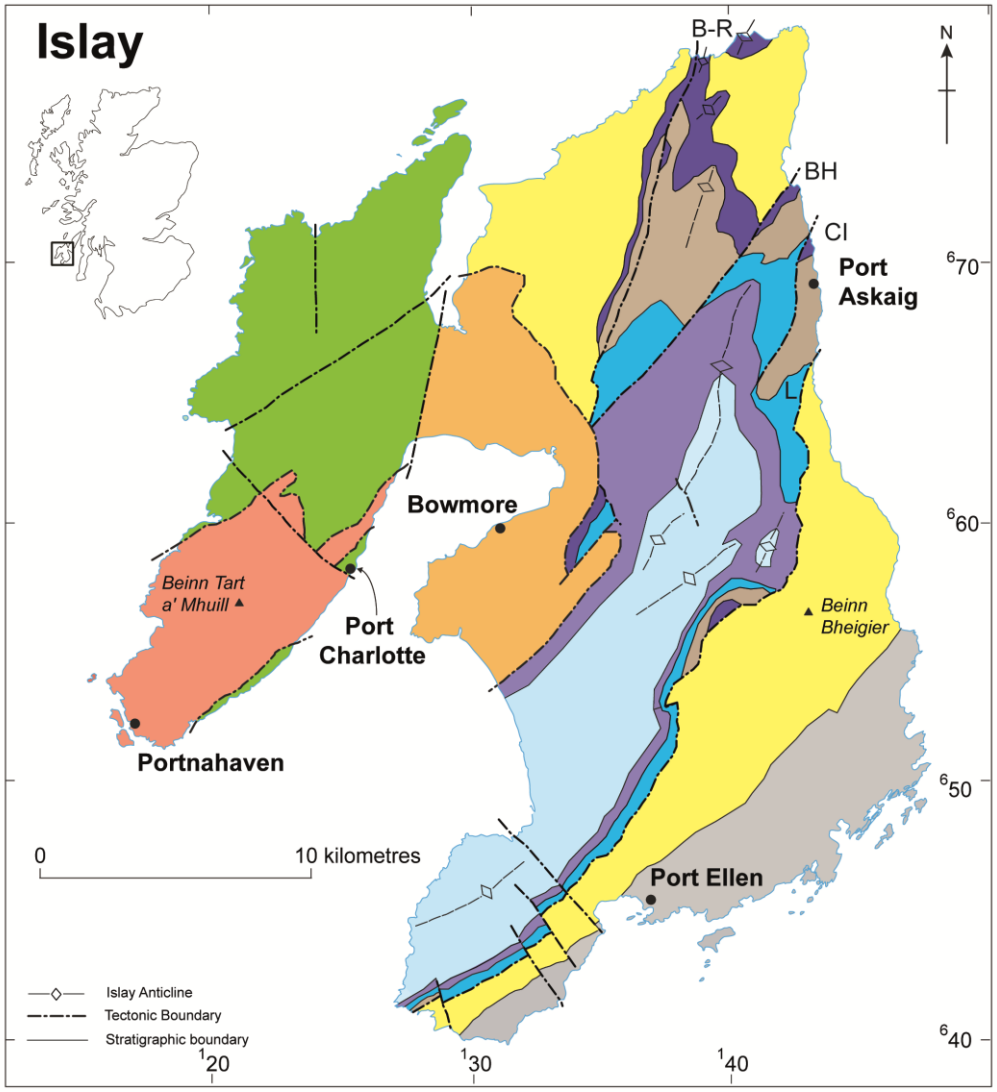

Generalised stratigraphic column